CHAPTER IV
STUDY OF NATURAL DYES FOR DYE-SENSITIZED SOLAR CELLS

4.1 Abstract

This work aims to study natural dyes which were used as the sensitizers for dye-sensitized solar cells (DSSCs). The optical properties of dyes solutions, mixed dyes solution and dyes on ZnO semiconductor were determined. Furthermore, adsorption studies which are kinetic adsorption and isothermal adsorption were studied. Four natural dyes which were yellow cotton flower, red orchid, spirulina and indigo, were investigated. The optical properties, kinetic and isothermal adsorption of natural dyes were measured using UV-Visible spectrometer. ZnO which was used as a semiconductor and fabricated by the doctor blade method was characterized using X-ray diffractometer. It was found that the maximum absorption wavelength of dyes in deionized water showed different wavelength which was 519, 620, 626 and 488 nm for red orchid, spirulina, indigo and yellow cotton, respectively. The maximum absorption wavelength of each dye on ZnO was shifted to higher wavelength (bathochromic shift) when compared with dyes solutions. For kinetic adsorption, the results showed that experimental data fitted with pseudo-second-order model. It indicated that dyes had chemical interaction with ZnO. Moreover, adsorption was promoted by both Langmuir model and Freundlich models. This can be explained that dyes adsorbed on ZnO using homogeneous monolayer and also heterogeneous multilayers.

4.2 Introduction

Dye sensitized solar cell (DSSC) is an attractive photovoltaic device due to low cost and relatively simple fabrication process. The semiconductors are one of components that used in DSSC photoanode. ZnO is one of the semiconductors and it is an attractive material in solar energy conversion due to its stability against photo corrosion and photochemical properties similar to TiO_2, having a band gap similar to TiO_2 at 3.2 eV and having higher electron mobility 115- 155 $cm^2/V\ s^2$ than that of

TiO_2 (Chou *et al.*, 2007). In addition, dye or the sensitizer is an essential component of DSSC that is used to enlarge the spectral absorbance. The sensitizer can be divided into two kinds, synthetic dyes and natural dyes. The synthetic dyes as ruthenium polypyridyl complexes are mostly used, and the result was obtained with the maximum conversion efficiency of 11% (Grätzel, 2005). However, the cost of synthetic dyes and environment effect are concerned, natural dyes have been applied to DSSC. The natural dyes that found in plant, fruits and other natural products show various colors and contain several pigments that can be easily extracted and then employed in DSSC. Chang and co-workers prepared TiO_2 DSSC by using pomegranate leaf and mulberry fruits as dye-sensitizers and the conversion efficiency of fabricated DSSC were 0.597% and 0.548%, respectively (Chang *et al.*, 2010). Wongcharee and co-workers have fabricated solar cells using natural dyes extracted from rosella, blue pea and a mixture of the extracts and has reported the efficiency of 0.37%, 0.05% and 0.15%, respectively (Wongcharee *et al.*, 2007). Therefore, study of adsorption mechanism of natural dyes on ZnO is an approach to understand their effect on efficiency in DSSC.

In order to study adsorption mechanism of dye that enhances the efficiency of solar cell, the natural dyes that extracted from red orchid, spirulina, indigo and yellow cotton were investigated. The optical properties of dyes and dyes on ZnO were determined using UV-Visible spectrophotometer. Moreover, the adsorption mechanism was studied that can be divided into two sessions: kinetics adsorption and isothermal adsorption. Finally, the conversion efficiency of DSSC was measured using Digital Keithley 2400 multimeter.

4.3 Experimental

4.3.1 Materials

Red orchid was purchased from Pak-Khlong market, Bangkok, Thailand. Spirulina powder was purchased from Phu-Fah store in Jatujak market, Thailand. Indigo powder was purchased from Baan Tum-Tao, Sakonnakhon, Thailand. Yellow cotton flower was collected from Nakhon Nayok, Thailand. A commercial ZnO nanoparticle (ZoNoP®, 99.93% ZnO) was purchase from Nano

Materials Technology Co., Ltd., in Thailand. Acetylacetone (≥ 99.5%) was purchased from Fluka. Triton X-100 (laboratory grade) was purchased from Acros Organics. Polyethylene glycol (PEG, MW 20,000), Lithium iodide beads (99%), 4-tert-butyl pyridine (96%) and hydrogen hexachloroplatinate (IV) hydrate (~38% Pt basis) were purchased from Aldrich. Iodine was purchase from Suksapan panit, Thailand. Fluorine-doped SnO_2 (FTO) glass (sheet resistance of 8 Ω/cm^2) was purchased from Dyesol Company.

4.3.2 Preparation of Natural Dye Sensitizers

Spirulina powder and indigo powder were used as received. Yellow cotton flower and red orchid were cut into small pieces and extracted by using deionized water. The solutions were freezed and dried via freeze-drying process. Then solid dyes were crushed and sieved before used. Finally, each dye powder was dissolved in water to obtain concentration of 10 g/L before used.

4.3.3 Preparation of ZnO for Doctor-blade Method

In order to prepare electrodes, the fluorine-doped SnO_2 (FTO) glass plates were washed with water and ethanol, respectively. The FTO-glass plates were fixed area by using transparent tape (size 1.0 cm x 1.0 cm). 1.0 g of ZnO nanoparticles was added into the 5.0 ml of PEG aqueous solution (0.1 g/ml) mixed with 0.1 ml of acetylacetone and 0.4 ml of triton X-100. The mixture was stirred for 1 day then it was extended onto the marked FTO-glass plates and calcined at 550 °C for 1 h to obtain the photoanode film. Then 1 ml of natural dye solutions was dropped on the cooled ZnO film at room temperature for 3 h. The excess dye molecules were washed out with water.

4.3.4 Preparation of Pt Electrode

The Pt electrode was prepared by doctor blade method. The 7 mM of hexachloroplatinic acid in 2-propanol were dropped and spread on FTO-glass which was marked area by using transparent tape (size 0.5 cm x 1.5 cm). Finally, it was calcined at 450 °C for 30 min.

4.3.5 Fabrication of DSSC

In order to fabricate the DSSC, the 127 μm-thick transparent parafilm® was inserted between photoanode and cathode to prevent the short circuit current by attaching on four edges of photoanode film and the Pt electrode was covered on the top. The redox electrolyte solution contained with 0.025 M of iodine (I_2), 0.5 M of lithium iodide (LiI) and 0.2 M of *tert*-butyl pyridine that was dissolved in acetonitrile. Then, the electrolyte was injected in between two electrodes.

4.3.6 Batch Adsorption Studies

For adsorption kinetics studies, 0.1 g of ZnO as absorbent was added to tubes containing 1 mL of dyes in deionized water with initial concentration at 100 mg/L. The concentrations of dye were monitored at different time intervals (from 60 to 600 min). For adsorption isotherms, the different initial concentrations of dye in deionized water were prepared (10-1200 mg/L). ZnO absorbent was immersed in dye solution until equilibrium was reached. The concentrations of dye were determined at the maximum wavelength using UV-Visible spectrometer.

4.3.7 Characterizations

The surface morphology and particle size of ZnO which was fabricated by doctor blading method and calcined at 550 °C was examined by X-ray diffractometer (XRD) with 2 theta (2θ) 20-70 degree and Field Emission Scanning Electron Microscope (FE-SEM).

The optical absorption of dyes in deionized water (2.5 g/L), extinction coefficient and dyes on ZnO were measured by a UV-Visible spectrophotometer (UV-1800) and UV-Visible spectrophotometer (UV-2500), respectively.

The batch adsorption of natural dyes was studied using UV-Visible spectrophotometer (UV-1800) at maximum absorption wavelength of each dye.

The photovoltaic properties of DSSC, short circuit current (J_{sc}, mA/cm^2), open circuit voltage (V_{oc}, V), fill factor (*FF*, %) and efficiency (η, %), which were calculated from J-V characteristic curve were determined by a digital

Keithley 2400 multimeter under an irradiation of white light from 100 mW/cm^2 halogen-tungsten lamp.

4.4 Results and discussion

4.4.1 Absorption Spectrum of Dyes Solution

Figure 4.1 showed the absorption spectrum of four natural dyes in deionized water. The dark blue pigment of indigo dye is indigo showed the maximum absorption wavelength at 626 nm (Jacquemin *et al.*, 2006). The red pigment of red orchid which is pelargonidin showed the maximum absorption wavelength at 519 nm (Tatsuzawa *et al.*, 2004). The yellow pigment of yellow cotton flower which is quercetin showed the absorption wavelength at 420 and 488 nm (Lu *et al.*, 2011). The green pigment of spirulina dye is *c*-phycocyanin showed the maximum absorption wavelength at 620 nm (Raghavarao, 2007). From the UV spectrum, their absorption is attributed to different chemical component of natural dyes. Furthermore, the extinction coefficient of each dye gave different value that it is depends on type of dyes. The highest extinction coefficient was spirulina followed yellow cotton, indigo and the lowest extinction coefficient was red orchid.

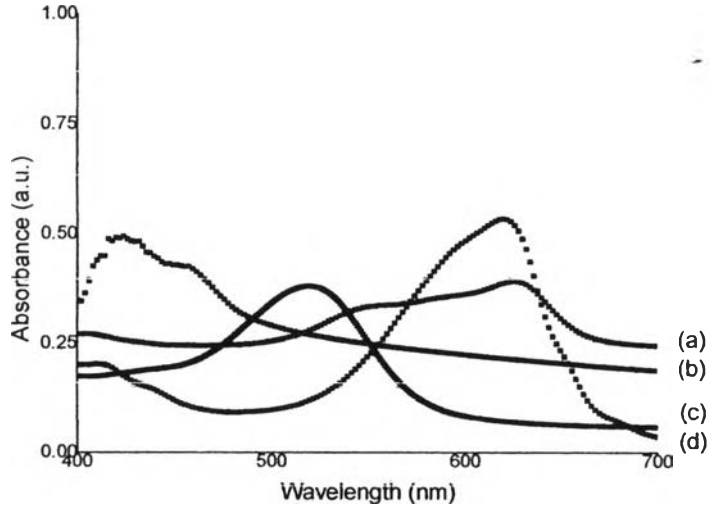

Figure 4.1 UV-Visible absorption spectrum of natural dyes solution: (a) indigo, (b) yellow cotton flower, (c) red orchid and (d) spirulina.

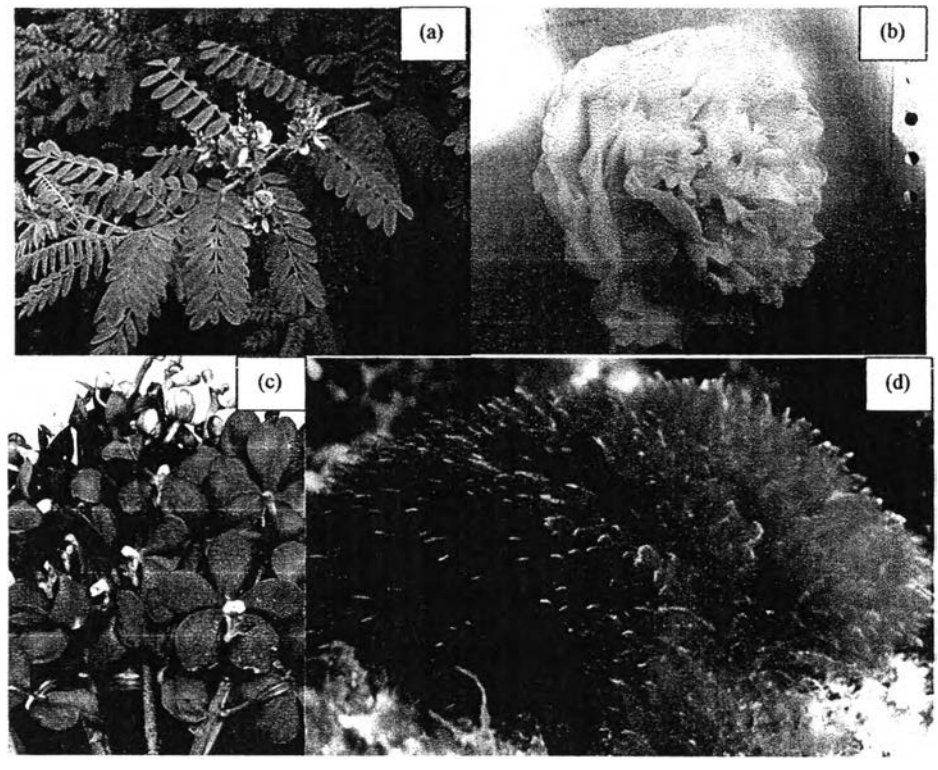

Figure 4.2 Photographic images of (a) indigo (http://www.indusladies.com/forums /hair-care-and-hair-styles/175367-wants-to-know-meaning-indigo.html), (b) yellow cotton flower, (c) red orchid and (d) spirulina (http://terranut.com/about/spirulina-health-benefits/).

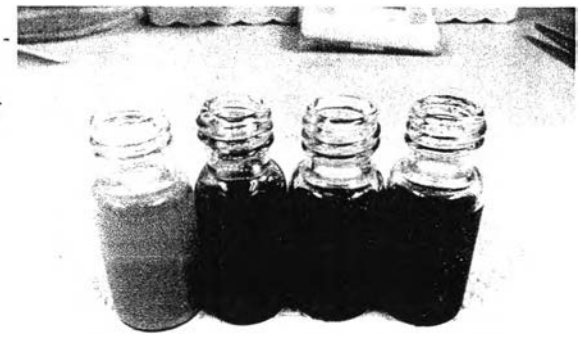

Figure 4.3 Photographic images of dyes solution from left to right; yellow cotton, spirulina, indigo and red orchid, respectively.

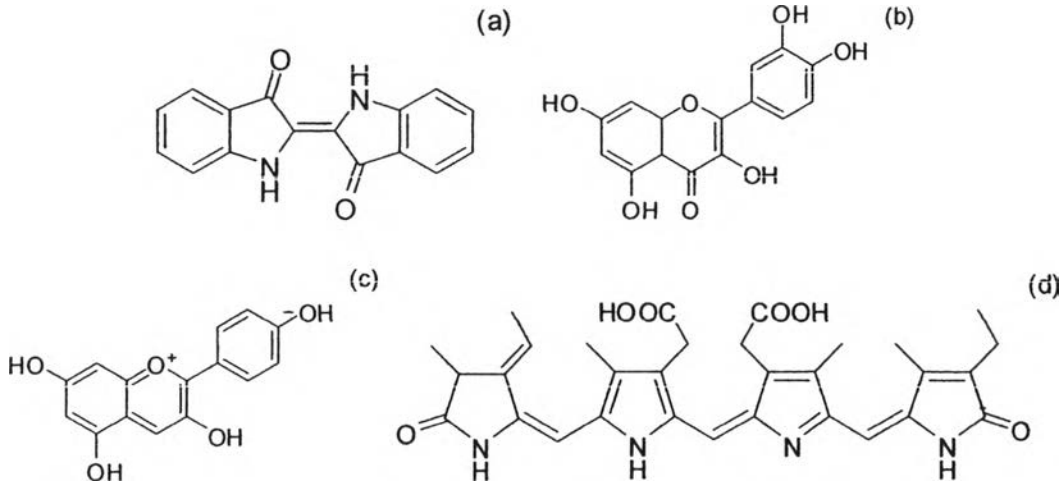

Figure 4.4 Photographic images of their molecular structures; (a) indigo (indigo), (b) yellow cotton flower (quercetin) , (c) red orchid (pelargonidin) and (d) spirulina (*c*-phycocyanin).

Table 4.1 Extinction coefficient of four natural dyes in deionized water

Natural dyes	**Extinction coefficient (L g^{-1} cm^{-1})**
Indigo	0.078
Red orchid	0.076
Spirulina	0.107
Yellow cotton flower	0.098

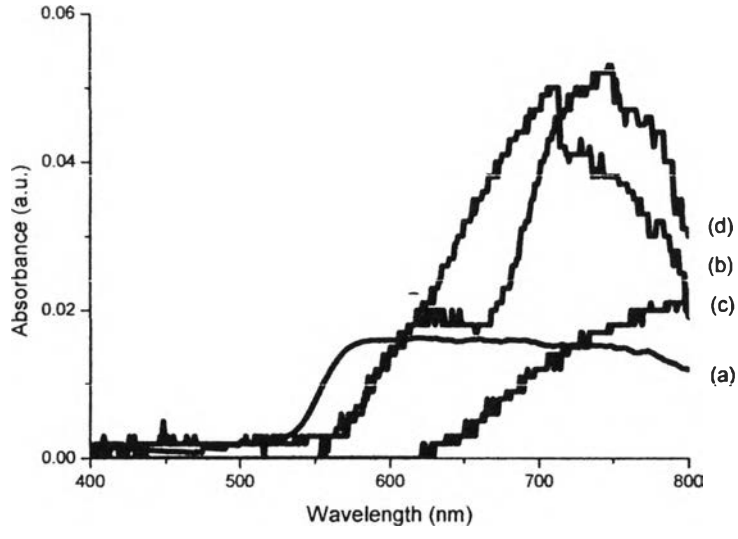

Figure 4.5 UV-Visible absorption spectra of natural dyes on ZnO. (a) Indigo, (b) yellow cotton flower, (c) red orchid and (d) spirulina.

Figure 4.5 showed the absorption intensity of natural dyes which absorbed on ZnO semiconductor. Maximum absorption intensity of yellow cotton, red orchid and spirulina was shift to higher wavelength (bathochromic shift) or called "red shift" when compared with UV-Visible spectrum of natural dye solution. This result can be explained that molecular interaction such as π-π stacking, electrostatic interaction or hydrogen bonding was occur between ZnO and natural dyes and π conjugation of the molecule was enlarged. When shift value is higher that mean the interaction was stronger (Ye *et al.*, 2012). In case of indigo, the maximum absorption on ZnO was about the maximum absorption of solution. Therefore, indigo dye had not any interaction with ZnO.

4.4.2 FT-IR Spectroscopy

The FT-IR spectral features of dyes and dyes/ZnO in KBr pellet was shown in Figure 4.6 For pelargonidin of red orchid, the band at 1600 cm^{-1} is assigned to C=O stretching. The band at 1500 cm^{-1} is assigned to C-C stretching. For the

higher wavenumbers, the broad band around 3400 cm^{-1} is assigned to O-H stretching (Mazzaracchio *et al.*, 2011).

For *c*-phycocyanin of spirulina, the bands at 1720 cm^{-1} and 1650 cm^{-1} is assigned to C=O stretching of carboxylic and amide group, respectively. For the higher wavenumbers, the broad band around 3250 cm^{-1} is assigned to O-H stretching of carboxylic group (Chakdar *et al.*, 2013).

For indigo, the bands at 1710 cm^{-1} and 1500 cm^{-1} is assigned to C=O stretching and C-C stretching in aromatic rings, respectively (Fiedler *et al.*, 2011). For the higher wavenumbers, the broad band around 3400 cm^{-1} with low intensity appears due to the moisture.

For quercetin of yellow cotton, the bands between the wavenumbers of 1800 and 750 cm^{-1} (FT-IR "finger print" region) reflect the primary biochemical and macronutrient components such as carbohydrates and lipids. The band at 1720 cm^{-1} is assigned to C=O stretching of main structure. The band at 1650 cm^{-1} is assigned to ring C-C stretching of phenyl ring. The band at 1030 cm^{-1} is assigned to the vibrational frequency of $-CH_2OH$ groups of carbohydrates. For the higher wavenumbers, the broad band around 3500 cm^{-1} is assigned to O-H stretching and the band at 2930 cm^{-1} is assigned to CH_2 anti-symmetric stretching of methyl groups mainly from lipids (Lu *et al.*, 2011).

Before the experiment, we expected that the spectrum of dye and dye/ZnO will give the divergent information due to the chemical bonding occurs between dye and ZnO. From the experimental data, it was found that the spectrum between dye and dye on ZnO were not significantly different. Therefore, IR spectra can be used to describe only the functional group of natural dyes but cannot give more information about the chemical bond which occurs between ZnO and natural dyes.

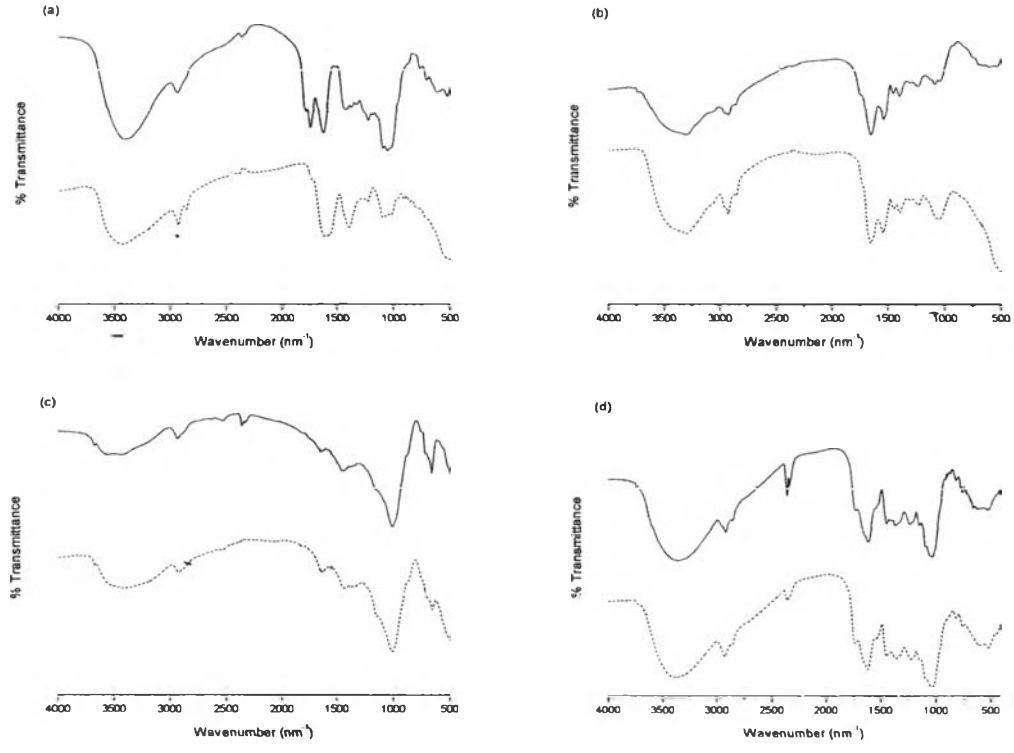

Figure 4.6 FT-IR spectra of dyes (—) and dyes on ZnO (- -) (a) red orchid, (b) spirulina, (c) indigo and (d) yellow cotton.

4.4.3 Surface Morphology and Characterization of ZnO by Doctor Blading Method

Figure 4.7 showed the XRD pattern of ZnO on FTO glass fabricated by doctor blade method. The XRD pattern corresponded to the hexagonal ZnO structure (wurzite) with the diffraction peaks of (100), (002), (101), (102) and (110) plane. The diffraction peaks at scattering angle 26.61, 37.85 and 51.62 degree corresponded to FTO (fluorine doped tin oxide) glass (Liao *et al.*, 2005).

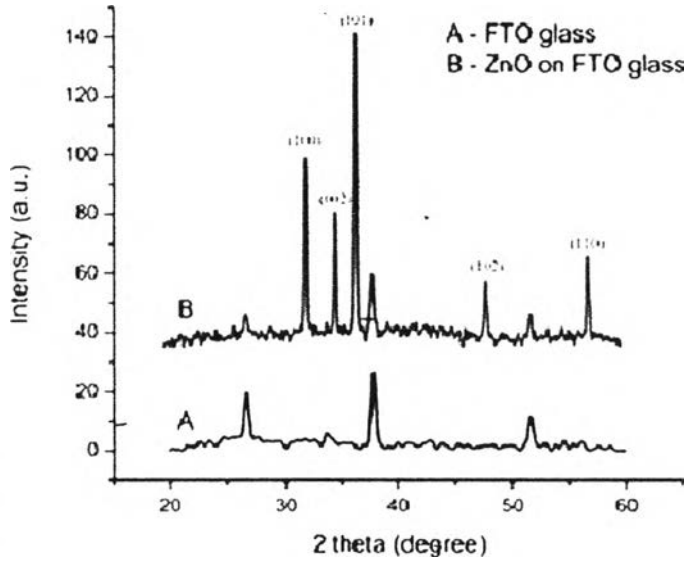

Figure 4.7 XRD pattern of ZnO film fabricated by doctor blade method.

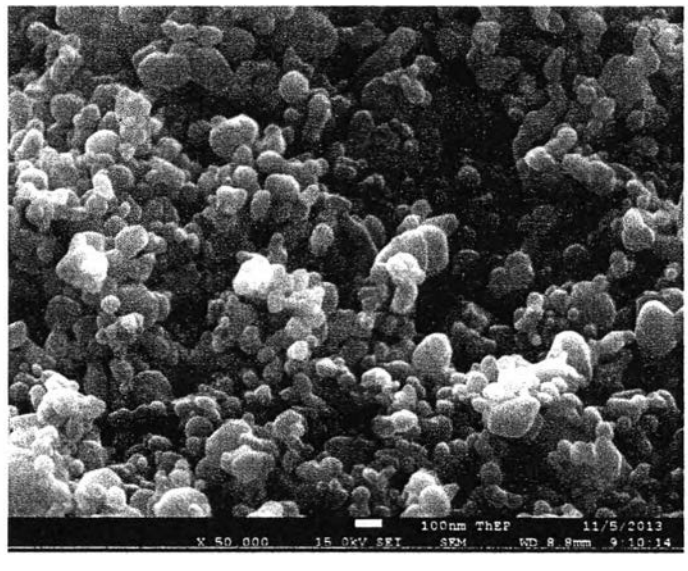

Figure 4.8 Cross-section FE-SEM image of ZnO film.

Figure 4.8 showed the cross section FE-SEM image of ZnO coated on FTO glass prepared by doctor blade method. The image revealed the particle size of ZnO about 92 nm and showed the porous structure of ZnO film due to the evaporation of organic solvent at high temperature, organic additive (acetyl acetone),

binder (polyethylene glycol, PEG) and surfactant (Triton X-100). Furthermore, the organic solvent was added into the ZnO paste for prevent the coagulation and cracking in ZnO electrode that influences the efficiency of DSSC (Saito *et al.*, 2009).

4.4.4 Kinetic Adsorption Studies

The study of kinetic adsorption, pseudo-first-order and pseudo-second-order, were used to describe the adsorption process at the solid-solution interface. The rate of removal of each dye by adsorption was dramatic initially and then slowed gradually until it reached an equilibrium following the Figure 4.9

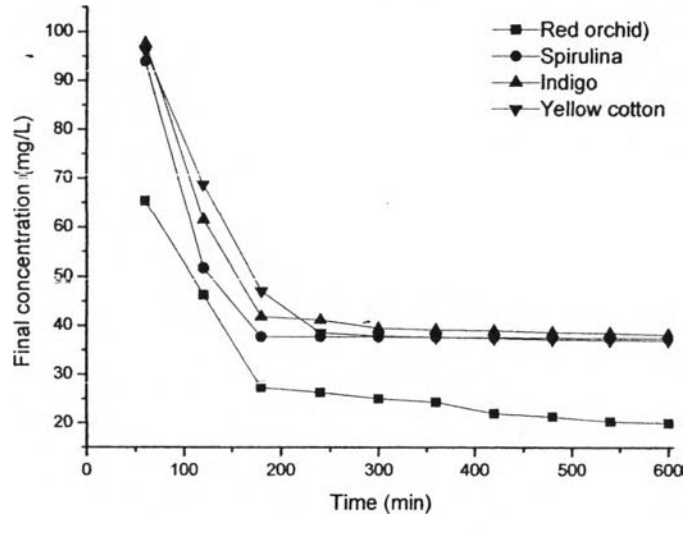

Figure 4.9 Effect of interval time of each dye onto ZnO (C_0 = 100 mg/L, T = 25°C).

The amount of dyes adsorbed onto ZnO semiconductor was calculated by the following mass balance relationship (Carpiné *et al.*, 2013) as:

$$q_e = (\frac{C_0 - C_e}{m})V \quad \textbf{(1)}$$

$$q_t = (\frac{C_0 - C_t}{m})V \quad \textbf{(2)}$$

Where C_o is the initial concentration of dyes (mg/L), C_t is the concentration of dyes at various time t (min), m is the weight of the ZnO or adsorbent (g) and V is the volume of dye solution (L).

In order to calculate the adsorption kinetic of dyes onto ZnO, the reaction will be assumed that adsorption is a pseudo-chemical reaction process. The pseudo-first-order rate expression of Lagergren and the pseudo-second-order kinetic model (El-Bindary *et al.*, 2014) are given as:

$$\log(q_e - q_t) = logq_e - k_1 t \quad \textbf{(3)}$$

$$t/q_t = 1/k_2 q_e^2 + 1/q_e t \quad \textbf{(4)}$$

Where q_t is the amount of dye adsorbed on adsorbent (mg/g) at various times t, q_e is the amount of dye adsorbed on adsorbent at equilibrium (mg/g), k_1 is the pseudo-first-order rate constant (min^{-1}) and k_2 is the pseudo-second-order rate constant (g mg^{-1} min^{-1}).

The corresponding kinetic constants which were q_e, k_1, k_2 were shown in Table 4.2 Moreover, the correlation coefficients: R_1^2 and R_2^2 were provided as the same table.

Table 4.2 Kinetic parameters of kinetic models for the adsorption of natural dyes onto ZnO semiconductor

Natural dyes	Models	Parameters	Values
Red orchid	Pseudo-first-order	q_e (mg/g)	1.2272
		k_1 (min^{-1})	0.0090
		R_1^2	0.2811
	Pseudo-second-order	q_e (mg/g)	14.0160
		k_1 (min^{-1})	0.0621
		R_2^2	0.9563
Spirulina	Pseudo-first-order	q_e (mg/g)	2.1117

		k_1 (min^{-1})	0.0190
		R_1^2	0.2997
	Pseudo-second-order	q_e (mg/g)	16.7060
		k_1 (min^{-1})	0.0678
		R_2^2	0.7256
Indigo	Pseudo-first-order	q_e (mg/g)	1.4818
		k_1 (min^{-1})	0.0109
		R_1^2	0.0386
	Pseudo-second-order	q_e (mg/g)	31.6150
		k_1 (min^{-1})	0.0802
		R_2^2	0.7586
Yellow cotton	Pseudo-first-order	q_e (mg/g)	1.4567
		k_1 (min^{-1})	0.0063
		R_1^2	0.9963
	Pseudo-second-order	q_e (mg/g)	36.1269
		k_1 (min^{-1})	0.0057
		R_2^2	0.8501

The correlative coefficients (R_1^2) of natural dyes for the pseudo-first-order kinetic model were between 0.0386 and 0.9963. The correlation coefficients (R_2^2) of natural dyes for the pseudo-second-order kinetic model are between 0.7256 and 0.9563. The correlation coefficients of the pseudo-second-order were more than correlation coefficients of pseudo-first-order. Therefore, the adsorption process of this study is not follow a pseudo-first-order reaction but it follows the pseudo-second-order kinetic model. It was noted that the process depends on both the amount of adsorbent and the amount of dye. So it can be concluded that some chemical interaction occurs between adsorbent and dye.

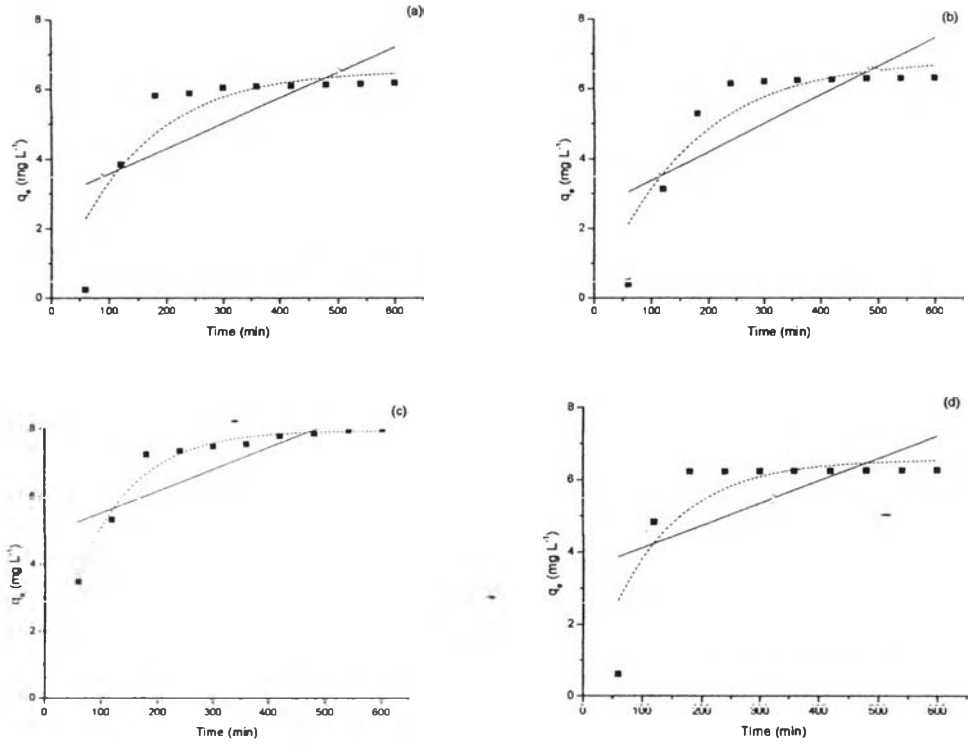

Figure 4.10 Experimental data (■), pseudo-first-order (—) and pseudo-second-order (- -) of (a) indigo, (b) yellow cotton, (c) red orchid and (d) spirulina on ZnO.

4.4.5 Isothermal adsorption studies

The main factors that describe the interactions for adsorption of dye are charge and structure of dye, adsorbent surface properties, hydrophobic and hydrophilic nature, hydrogen bonding, electrostatic interaction, steric effect and van der Waal forces etc. (El-Bindary *et al.*, 2014). Equilibrium studies that give the capacity of the adsorbent and adsorbate are described by adsorption isotherm. This method is usually varying the concentration of adsorbate at fixed temperature. The equilibrium experimental data for natural dyes on ZnO was compared using two isotherm equations which are Langmuir and Freundlich.

Langmuir adsorption isotherm describes that the adsorption will occur at the outer sphere of adsorbent and solute will interact with adsorbent only homogeneous monolayer (El-Bindary *et al.*, 2014). Theoretically, the adsorbent has a

limited capacity for adsorbate. Therefore, the monolayer capacity can be represented as linear graph of Langmuir equation.

$$q_e = \frac{q_m K_L C_e}{1+K_L C_e} \quad (5)$$

Where C_e is the equilibrium concentration of dye (mg/L), q_e is the amount of dye adsorbed on adsorbent at equilibrium (mg/g), q_m is the monolayer capacity of dye adsorbed on adsorbent (mg/g) and K_L is the Langmuir adsorption constant (L/mg). When the equation is formatted to get the equation below

$$\frac{1}{q_e} = \frac{1}{q_m K_L}\frac{1}{C_e} + \frac{1}{q_m} \quad (6)$$

Freundlich isotherm is an empirical equation that describes heterogeneous systems. To characterize, heterogeneity factor ($1/n$) is determined. Heterogeneity factor describes reversible adsorption and the formation not only monolayer.

$$q_e = K_F C_e^{1/2} \quad (7)$$

Where q_e is the amount of dye adsorbed on adsorbent at equilibrium (mg/g), C_e is the equilibrium concentration of dye (mg/L), K_F is Freundlich constant (L g^{-1}) and $1/n$ is the heterogeneity factor. Therefore, a linear form of Freundlich equation can be obtained follow in equation 8.

$$\log q_e = \log K_F + \frac{1}{n}\log C_e \quad (8)$$

Therefore, the straight-line plots of equation 6 for Langmuir isotherm and equation 8 for Freundlich isotherm will give the parameters following table 4.3

Table 4.3 Langmuir and Freundlich parameters for the adsorption of natural dyes onto ZnO semiconductor

Natural dyes	Models	Parameters	Values
Red orchid	Langmuir	q_m	18.4502
		K_L	5.5949×10^{-5}
		R_1^2	0.9704
	Freundlich	K_F(L/g)	0.0580
		N	0.7655
		R_2^2	0.9735
Spirulina	Langmuir	q_m	14.3062
		K_L	0.0010
		R_1^2	0.9591
	Freundlich	K_F(L/g)	0.1612
		N	1.0848
		R_2^2	0.9581
Indigo	Langmuir	q_m	11.7827
		K_L	0.0016
		R_1^2	0.9591
	Freundlich	K_F(L/g)	0.1951
		N	1.1592
		R_2^2	0.9581
Yellow cotton	Langmuir	q_m	24.0384
		K_L	0.0005
		R_1^2	0.9787
	Freundlich	K_F(L/g)	0.1040
		N	0.9229
		R_2^2	0.9802

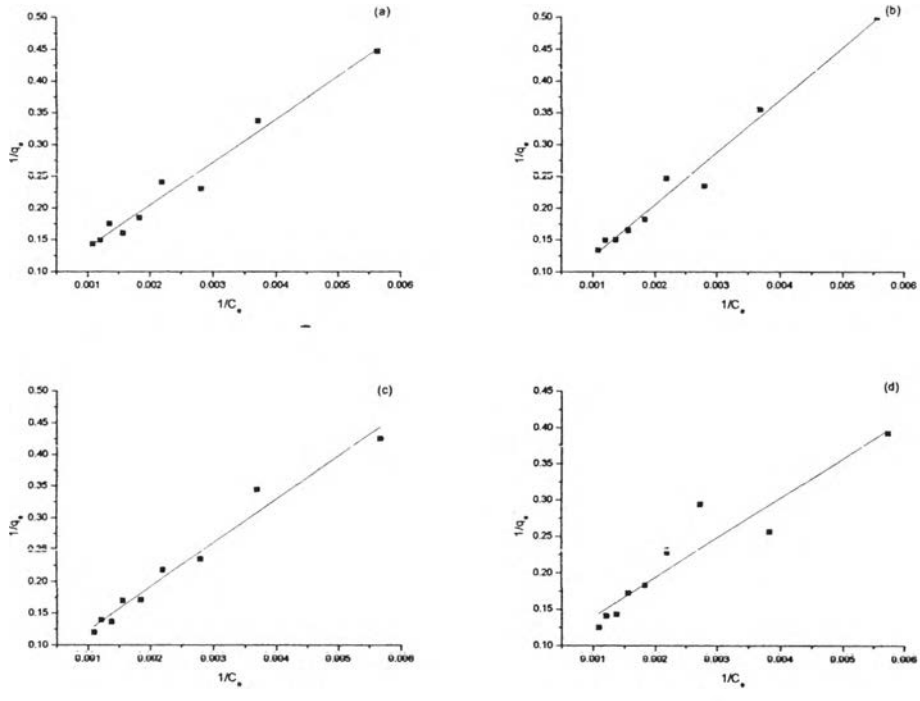

Figure 4.11 Langmuir plots for adsorption of (a) indigo, (b) yellow cotton, (c) red orchid and (d) spirulina on ZnO.

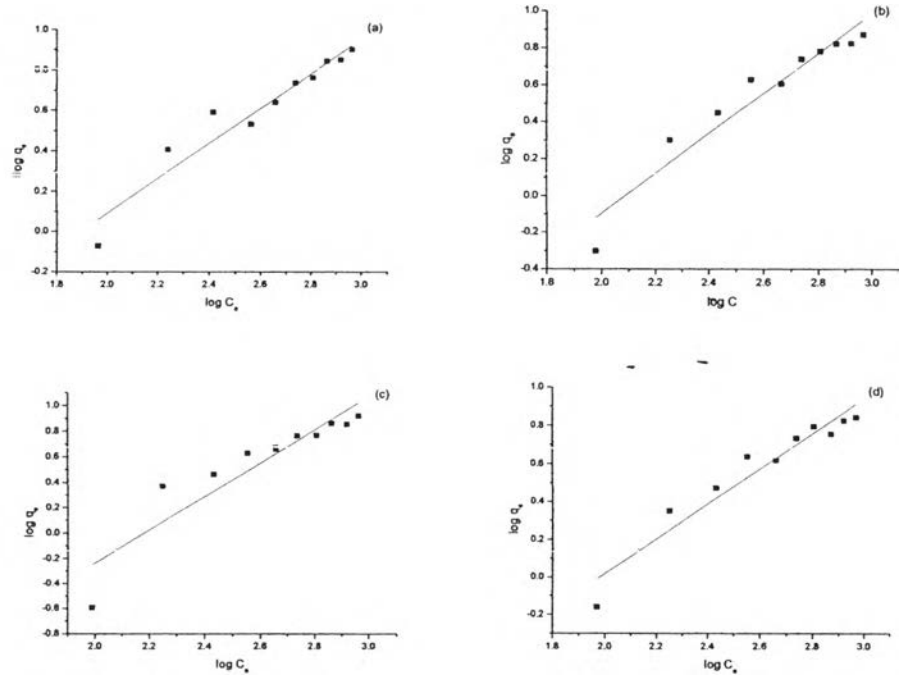

Figure 4.12 Freundlich plots for adsorption of (a) indigo, (b) yellow cotton, (c) red orchid and (d) spirulina on ZnO.

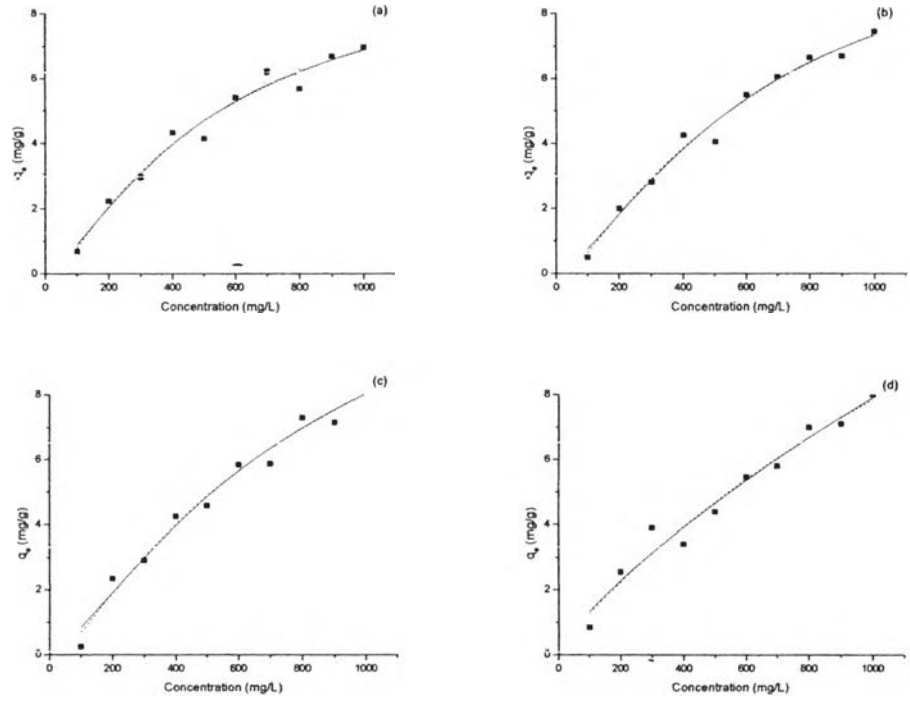

Figure 4.13 Experimental data (■), Langmuir model (—) and Freundlich model (- -) of (a) indigo, (b) yellow cotton, (c) red orchid and (d) spirulina on ZnO.

The experimental data showed that the correlation coefficients (R_1^2) values of Langmuir model of Freundlich model were similar to the correlation coefficients (R_2^2). This result indicated that all dyes had homogeneous monolayer interaction at outer sphere worked together with heterogeneous multilayers. Moreover, adsorption was more favorable when $1 < n < 10$ (Satyanarayana *et al.*, 1999) than desorption. For n value, indigo showed the higher value than other dyes. This meant that adsorption capacity of indigo onto ZnO was highest.

4.4.6 Performance of Natural DSSCs

Figure 4.16 showed J-V characteristic curves of DSSC that sensitized with natural dyes. Table 4.4 showed the data acquired from measuring the photoelectric conversion efficiency of DSSC. The highest efficiency of DSSC which was prepared by indigo dye was 0.020% with short-circuit current (J_{sc}) of 0.426

mA/cm^2, open circuit voltage (V_{oc}) of 0.234 and fill factor of 20.1. The minimize efficiency of DSSC prepared by red orchid is 0.0005 %. The DSSC prepared from indigo dye showed the highest efficiency because indigo had broad absorption more than other dyes causing produced more electron and resulted in highest J_{sc} value. Moreover, this was noted that the indigo was the best electron donor when compared with the others. In addition, indigo had the highest adsorption capacity onto ZnO causing why the DSSC based on indigo dye had the highest conversion efficiency.

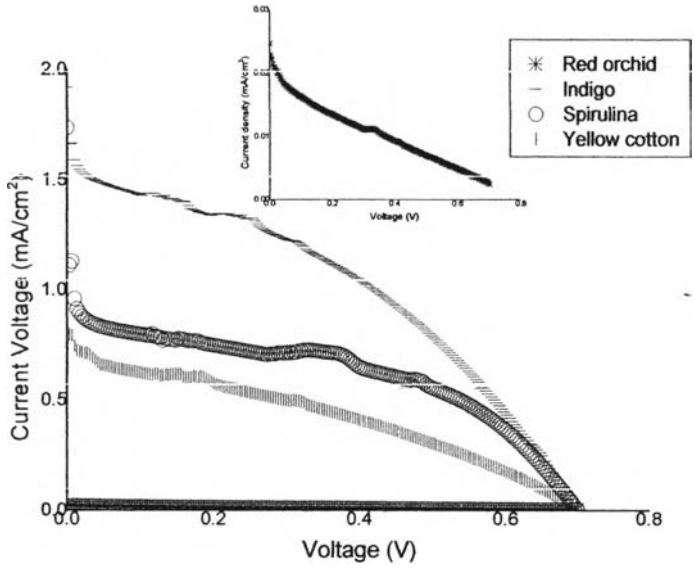

Figure 4.14 The J-V characteristics of DSSC with natural dyes. Inset showed the enlarged curve of red orchid dye.

Table 4.4 The efficiency parameters of DSSC with natural dyes

Natural dyes	J_{sc} (mA/cm^2)	V_{oc} (V)	FF (%)	η (%)
Indigo	0.426	0.234	20.1	0.0200
Red orchid	0.013	0.368	14.8	0.0005
Spirulina	0.039	0.507	15.6	0.0171
Yellow cotton flower	0.203	0.168	11.4	0.0041

4.5 Conclusions

In summary, the optical properties and absorption mechanism of all dyes was studied. For optical properties, the maximum absorption of red orchid, spirulina, indigo and yellow cotton in deionized water was 519, 620, 626 and 488 nm, respectively. Furthermore, the maximum absorption of each dye on ZnO was different when compared with dyes solution. From experimental data, the maximum absorption was shift to higher wavelength which was called bathochromic shift or red shift because of molecular interaction between ZnO and dyes. Moreover, kinetic adsorption and isothermal adsorption were studied to ensure the result in the optical properties. The pseudo-first-order and pseudo-second-order were the model which used to study the kinetic adsorption of dyes on ZnO. The result showed that all dyes were fitted to pseudo-second-order more than pseudo-first-order. It indicated that the interaction of all dyes was chemical adsorption process. For isothermal adsorption, the Langmuir model and Freundlich model were used to study how dyes interacted with ZnO. The isothermal adsorption result showed that correlation coefficient of Langmuir plot and Freundlich plot were significantly indifferent. Therefore, dyes interacted with ZnO homogeneous monolayer at outer sphere and also heterogeneous multilayers. Moreover, the n values showed that indigo had the highest adsorption capacity. This caused the conversion efficiency of DSSC based on indigo had the highest value.

4.6 Acknowledgements

The author gratefully thanks the Petroleum and Petrochemical College, Chulalongkorn University for the chemical and equipment laboratory support.

4.7 References

Carpiné, D., Dagostin, J. L. A., Silva, V. R. d., Igarashi-Mafra, L.,Mafra, M. R. (2013) Adsorption of volatile aroma compound 2-phenylethanol from

synthetic solution onto granular activated carbon in batch and continuous modes. Journal of Food Engineering, 117, 370-377.

Chakdar, H., Saha, S.,Pabbi, S. (2013) Chromatographic and spectroscopic characterization of phycocyanin and its subunits purified from Anabaena variabilis CCC421. Applied Biochemistry and Microbiology, 50(1), 62-68.

Chang, H.,Lo, Y. J. (2010) Pomegranate leaves and mulberry fruit as natural sensitizers for dye-sensitized solar cells. Solar Energy, 84(10), 1833-1837.

Chou, T. P., Zhang, Q. F.,Cao, G. Z. (2007) Effects of dye loading conditions on the energy conversion efficiency of ZnO and TiO2 dye-sensitized solar cells. Journal of physical Chemistry C, 111(50), 18804-18811.

El-Bindary, A. A., Diab, M. A., Hussien, M. A., El-Sonbati, A. Z.,Eessa, A. M. (2014) Adsorption of Acid Red 57 from aqueous solutions onto polyacrylonitrile/activated carbon composite. Spectrochimica Acta. Part A: Molecular and Biomolecular Spectroscopy, 124C, 70-77.

Fiedler, A., Baranska, M.,Schulz, H. (2011) FT-Raman spectroscopy-a rapid and reliable quantification protocol for the determination of natural indigo dye in Polygonum tinctorium. Journal of Raman Spectroscopy, 42(3), 551-557.

Grätzel, M. (2005) Solar energy conversion by dye-sensitized photovoltaic cells. Inorganic Chemistry, 44(20), 6841-6851.

Jacquemin, D., Preat, J., Wathelet, V.,Perpète, E. A. (2006) Substitution and chemical environment effects on the absorption spectrum of indigo. The Journal of Chemical Physics, 124(7), -.

Liao, J. Y.,Ho, K. C. (2005) A photovoltaic cell incorporating a dye-sensitized ZnS/ZnO composite thin film and a hole injecting PEDOT layer. Solar Energy Materials and Solar Cells, 86, 229-241.

Lu, X., Ross, C. F., Powers, J. R.,Rasco, B. A. (2011) Determination of quercetins in onion (Allium cepa) using infrared spectroscopy. Journal of Agricultural and Food Chemistry, 59(12), 6376-6382.

Mazzaracchio, P., Tozzi, S., Boga, C., Forlani, L., Pifferi, P. G.,Barbiroli, G. (2011) Interaction between gliadins and anthocyan derivatives. Food Chemistry, 129(3), 1100-1107.

Raghavarao, G. (2007) Aqueous two phase extraction for purification of C-phycocyanin. Biochemical Engineering Journal, 34, 154-164.

Saito, M.,Fujihara, H. (2009) Fabrication and photovoltaic properties of dye-sensitized ZnO thick films by a facile doctor-blade printing method using nanocrystalline pastes. Journal of the Ceramic Socir=ety of Japan, 117(7), 823-827.

Satyanarayana, J., Murthy, G. S.,Sasidhar, P. (1999) Adsorption studies of caesium on zirconium molybdoarsenate (ZrMAs). Waste Management, 19(6), 427-432.

Tatsuzawa, F., Saito, N., Seki, H., Yokoi, M., Yukawa, T., Shinoda, K.,Honda, T. (2004) Acylated anthocyanins in the flowers of *Vanda* (Orchidaceae). Biochemical Systematics and Ecology, 32, 651-664.

Wongcharee, K., Meeyoo, V.,Chavadej, S. (2007) Dye-sensitized solar cell using natural dyes extracted from rosella and blue pea flowers. Solar Energy Materials and Solar Cells, 91(7), 566-571.

Ye, T. X., Ye, S. L., Chen, D. M., Chen, Q. A., Qiu, B.,Chen, X. (2012) Spectroscopic characterization of tetracationic porphyrins and their noncovalent functionalization with graphene. Spectrochimica Acta. Part A: Molecular and Biomolecular Spectroscopy, 86, 467-471.